Raman scattering of orthorhombic and tetragonal $Ln_2NiO_{4+\delta}$ (Ln identical to La,Pr,Nd) oxides

Raman scattering of orthorhombic and tetragonal Ln$_2$NiO$_{4+\delta}$ (Ln $\equiv$ La, Pr, Nd) oxides

A de Andres†, M T Fernandez-Diaz†, J L Martinez†,
J Rodriguez-Carvajal‡, R Saez-Puche§ and F Fernandez§

† Instituto de Ciencia de Materiales de Madrid, Consejo Superior de Investigaciónes Científicas, Universidad Autónoma de Madrid, Departamento Física Aplicada C-IV, Madrid E-28049, Spain
‡ Instituto de Ciencia de Materiales de Barcelona, Consejo Superior de Investigaciónes Científicas, C/Martí i Franqués s/n, Barcelona E-08028, Spain
§ Departamento Química Inorgánica, Facultad de Ciencias Químicas, Universidad Complutense de Madrid, Madrid E-28040, Spain

Abstract. The vibrational properties of polycrystalline Ln$_2$NiO$_{4+\delta}$ (Ln $\equiv$ La, Pr and Nd) have been investigated by means of Raman scattering in samples with several oxygen contents ($\delta = 0$ and 0.15) at different temperatures (74 K < T < 250 K), and over a spectral range 50–5500 cm^{-1}. The factor group analysis predicts 18 Raman-active modes for the room-temperature phase of stoichiometric samples ($\delta = 0$, orthorhombic D$_{2h}^{18}$ (*Bmab*)). Nearly all the observed peaks have been identified with particular atomic displacements even if no selection rules can be applied in powder samples. Two large double-phonon peaks are observed and the dependence of the phonon frequencies on the Ln ion is studied. Two out of the four allowed modes for the oxidized compounds are identified together with some spurious peaks corresponding to defects in the lattice, probably due to randomly distributed interstitial oxygen atoms.

1. Introduction

The interest in the behaviour of Ln$_2$MO$_{4+\delta}$ (Ln $\equiv$ rare earth, M $\equiv$ Cu, Ni or Co) is very strong owing to the great variety of properties such as structural instabilities, magnetic ordering and superconducting states in the different compounds of the family. There are some properties which are shared by almost all compounds, e.g. the antiferromagnetic ordering of the 3d metal, the strong anisotropy in the magnetic and transport properties, and a dramatic dependence on the oxygen stoichiometry. The Ln$_2$CuO$_{4+\delta}$-type compounds have been studied in detail, because of the superconducting state present in some elements of the family at rather high temperatures. Information about the nickelates is much less complete, as is the case for the cobalt systems. The Ln$_2$NiO$_{4+\delta}$ systems have been studied for a long time, but most of the published information lacks proper characterization of the oxygen stoichiometry. This is mainly the reason why some properties are very difficult to understand. In well characterized Ln$_2$NiO$_{4+\delta}$ (Ln $\equiv$ La, Pr and Nd) samples, the structural and magnetic properties are highly related.

The Ln$_2$NiO$_4$ compounds present an orthorhombic structure at room temperature (RT) (space group, *Bmab*). At high temperatures there is a structural phase transition to the well known tetragonal K$_2$NiF$_4$-type structural space group *I4/mmm*. This phase

transformation has only been measured in La_2NiO_4 ($T_1 \approx 770$ K); in other cases the expected transition temperature is higher than the melting point. At low temperatures ($T <$ RT) there is a second structural transformation to another tetragonal phase (space group, $P4_2/ncm$). This transformation is of first-order type and is accompanied by the creation of local microstrains oriented along some specific directions. These microstrains make the local symmetry much closer to orthorhombic symmetry (space group $Pccn$). A detailed neutron diffraction study has been discussed in [1–4]. The main conclusion is that the average symmetry for neutrons is tetragonal but locally is closer to orthorhombic.

From the magnetic point of view, the Ln_2NiO_2 systems present a very rich phenomenology. The Ni ions order 3D antiferromagnetically at temperatures T_N (around 325 ± 5 K) independently of the rare-earth ion (La, Pr and Nd). The magnetic moments are along the a axis [1–4], and a strong two-dimensional character is expected. The low-temperature structural phase transition allows canting in the magnetic moments, which gives rise to a net ferromagnetic component. At lower temperatures, there is also the magnetic ordering of the rare-earth sublattice in a coupled magnetic structure for $Ln \equiv Nd$ and Pr [1, 2]. At intermediate temperatures, there is a complex in-plane spin reorientation of the Ni sublattice.

The lattice dynamics of the Ln_2MO_4 systems have only recently been initiated. One interesting result [5] is the soft mode associated with the tetragonal-to-orthorhombic transition in La_2CuO_4. The main phonon branches have also been measured by neutron scattering in La_2CuO_4 and in non-stoichiometric $La_{1.9}NiO_{3.87}$ [6]. All the frequencies of the phonon modes fit well in a simple shell model which reproduces the soft-mode behaviour [7]. Some workers [8, 9] have observed in the Raman spectra of tetragonal Ln_2CuO_4 ($Ln \equiv La$, Nd, Sm) the spin-pair excitations corresponding to a planar quantum antiferromagnet and obtained the exchange parameter J, which depends on the Cu–O distance.

The low-temperature phase transition has been reported in $(LaBa)_2CuO_4$ at 80 K [10], Nd_2NiO_4 at 125 K [1], La_2NiO_4 at 80 K [3, 4], Pr_2NiO_4 at 115 K [2] and La_2CoO_4 at 117 K [11]. The lattice dynamics associated with this transition have not been yet performed because of the lack of sizable single crystals for neutron scattering. Very recently some infrared (IR) absorption data on Ln_2NiO_4 with $Ln \equiv La$, Pr and Nd have been published [12]. The IR spectra showed, in relation to the phase transition, a mode splitting in the band associated with the Ni–O stretching in the equatorial plane of the Ni octahedra. Some Raman and IR spectroscopy data have been published for $La_2NiO_{4+\delta}$ [13] but the stoichiometry of this sample was not specified (it was very probably, well oxidized) and the Raman spectra presented are difficult to understand. Recently, Burns and Dacol [14] advise the possibility of *in situ* burning of the sample by the laser beam during the measurement procedure, producing the original oxides (Ln_2O_3). Recently, the Raman spectra of La_2CuO_4 have indicated a local symmetry breaking [15], because the high-temperature tetragonal phase showed phonon modes only allowed in an orthorhombic phase. It was argued that it is possible that antiferromagnetic fluctuations give rise to this local decrease in the symmetry. However, it may be possible that the high-temperature phase is averaged tetragonal but locally slightly orthorhombic, as is the case for the low-temperature tetragonal phase in the nickelates.

Our aim, in the present work, is to characterize the lattice dynamics for structurally well known $Ln_2NiO_{4+\delta}$ samples, and to discuss the effect of the oxygen doping as well as the low-temperature structure phase transition.

2. Experimental details

The samples were prepared using the standard ceramic method. The final result was the oxidized $Ln_2NiO_{4+\delta}$ compounds. The samples were subsequently pressed into pellets
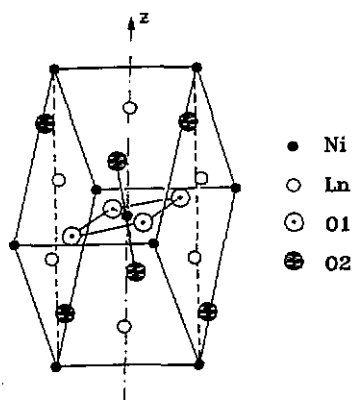
Figure 1. Primitive cell of the orthorhombic phase (*Bmab*) of the stoichiometric Ln_2NiO_4 compounds.

and sintered at a high temperature in air. In order to reach the ideal stoichiometry, each pellet was introduced, for a few hours, at 510 K into a dry hydrogen flow. In that way, two types of sample for each rare-earth ion—fully oxidized (black) and stoichiometric (yellowish-brown)—were obtained.

The Raman spectra were performed in the back-scattering geometry with an x–y Dilor spectrometer in the multichannel option. The excitation sources were the 488 and 514.5 nm lines of an Ar^+ Spectra Physics laser. The beam power on the samples was always less than 20 mW. The spectra of the stoichiometric samples were recorded at several temperatures between 230 and 74 K. The low temperature and low beam power prevent oxidation or damage of the samples which were in an Oxford Instruments flux cryostat with helium exchange gas. The spectra of the oxidized samples were also recorded at a low temperature (around 170 K), even if they do not present any phase transition, in order to prevent their heating. Surface darkening has been observed in the stoichiometric samples at the incident beam position when performing tests at room temperature and in a helium-deficient atmosphere.

3. Factor group analysis

While the most studied systems are the oxidized $Ln_2NiO_{4+\delta}$ which have been described as tetragonal with the *I4/mmm* space group, the stoichiometric samples ($\delta = 0$) present, at room temperature, the *Bmab* space group with four formulae per unit cell and antiferromagnetic ordering of the Ni sublattice. The three compounds La_2NiO_4, Pr_2NiO_4 and Nd_2NiO_4 undergo a structural phase transition, at 80 K, 115 K and 125 K, respectively, to another locally orthorhombic structure (*Pccn*), which is seen as a tetragonal averaged structure in neutron diffraction with the presence of microstrains following a particular *hkl*-dependence [3].

3.1. Stoichiometric samples

The RT point group is the centrosymmetric D_{2h} and the primitive cell (figure 1) contains 14 ions and 42 normal modes. The Ni ions are surrounded by distorted oxygen octahedra but the structure can also be seen as a stacking of alternating planes of nickel and oxygen ions of type 1 (O(1)) and planes of lanthanide ions (Ln) and oxygen ions of type 2 (O(2)). The site symmetry of the Ni is C_{2h} and has inversion symmetry so that the Ni

ions will not be involved in any Raman mode. The O(1) are on C_2 sites while the O(2) and the Ln ions are on equivalent sites (f) with C_s symmetry.

The irreducible representations of the 42 normal modes at $k = 0$ are

$$5A_g + 3B_{1g} + 4B_{2g} + 6B_{3g} + 4A_u + 7B_{1u} + 8B_{2u} + 5B_{3u}.$$

Among them, all the 18 even (g) modes are Raman active, the acoustic modes are $1B_{1u} + 1B_{2u} + 1B_{3u}$, and the $4A_u$ are silent; so 17 IR modes ($6B_{1u} + 7B_{2u} + 4B_{3u}$) are expected.

The low-temperature structure can be described in the tetragonal $P4_2/ncm$ (D_{4h}^{16}) space group, as seen by neutron diffraction, but strained in such a way that locally the lattice parameters a and b are slightly different, leading to the $Pccn$ (D_{2h}^{10}) group. The values of a and b fluctuates, along the sample, around the mean a of the tetragonal group [3]. The primitive cells of the two space groups contain 28 ions ($Z = 4$), which means that the cell is doubled below the phase transition, but the number of Raman-active modes predicted by the group theory is quite different in each group.

The irreducible representations at $k = 0$, for the orthorhombic group are

$$8A_g + 8B_{1g} + 10B_{2g} + 10B_{3g} + 11A_u + 11B_{1u} + 13B_{2u} + 13B_{3u}.$$

The point group is the same as before (D_{2h}) so that it has the same characteristics: the 36 even modes are Raman active (the A_g modes have the diagonal components of the polarizability tensor while the B_g modes have the non-diagonal components), the $11A_u$ are silent and the 34 odd modes are IR active.

The irreducible representations at the Γ point of the tetragonal group D_{4h}^{16} are

$$5A_{1g} + 3A_{2g} + 3B_{1g} + 5B_{2g} + 10E_g + 3A_{1u} + 8A_{2u} + 8B_{1u} + 3B_{2u} + 13E_u.$$

In this case, the A_{2g}, A_{1u}, B_{1u} and B_{2u} are silent modes and the acoustic modes are $1A_{2u} + 1E_u$, so that there are 23 Raman-active modes and 21 IR-active modes.

The site symmetry of the Ni ions is C_1 in the orthorhombic group and only keeps the inversion symmetry, while it remains C_{2h} in the tetragonal symmetry. In fact the structure is only slightly distorted in comparison with the RT structure and the two descriptions for the low-temperature structure are quite similar. The most remarkable feature is that the four O(1) in the Ni plane are no longer equivalent (they have been called O(1) and O(1')), and now there are two different distances to the Ni ion. The only difference between the tetragonal and orthorhombic groups is, taking into account that the z coordinate of the O(1) is nearly zero in the $Pccn$ symmetry, that the cell parameters a and b are equal or slightly different, respectively. When $a \neq b$ the $E_{g,u}$ modes are split into $1B_{2g,2u} + 1B_{3g,3u}$ modes. Nevertheless, the difference between the parameters a and b may be too small to induce an observable frequency splitting.

3.2. Oxidized samples

The oxidized $La_2NiO_{4+\delta}$ has the tetragonal $I4/mmm$ (D_{4h}^{17}) space group with two formulae in the unit cell and one in the primitive cell. Group theory predicts only $2A_{1g} + 2E_g$ Raman-active modes at the Γ point [13]. The symmetry is much higher than in the previous cases and only the O(2) and Ln ions can be involved in even normal modes. The other ions (O(1) and Ni) are in centrosymmetric sites.

The symmetry of the other two oxidized compounds is close to tetragonal but is not so clear with the data available [1, 2]. The problem arises because the smaller size of the rare-earth ions induces a more distorted structure with more room for interstitial oxygen
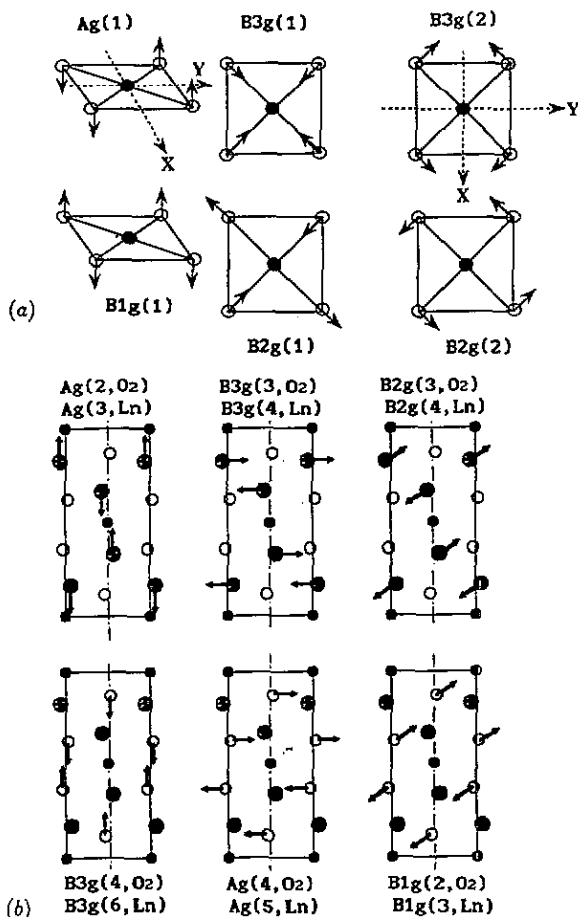
Figure 2. Atomic displacements of the normal modes of the *Bmab* phase.

ions. The final effect will be a tetragonal phase with many defects such as interstitial oxygen ions, or perhaps an orthorhombic (*Fmmm*) or even lower-symmetry phase with extra oxygen ions as well.

4. Lattice vibrational modes

4.1. Stoichiometric compounds

The atomic displacements of the Raman-active modes of the *Bmab* structure are shown in figure 2. The modes corresponding to vibrations of the NiO_2 layers $(1A_g(1) + 1B_{1g}(1) + 2B_{2g}(1, 2) + 2B_{3g}(1, 2))$ (figure 2(*a*)) consist basically of two Ni—O(1) stretchings, two Ni—O(2) bendings and two tilts of the oxygen squares. It is expected that the stretching modes will have the highest energy and the tilt modes the lowest. The $A_g(1)$ mode corresponds to the deformation from tetragonal (*I4/mmm*) to orthorhombic (*Bmab*) and therefore will have the lowest energy.

Figure 2(*b*) shows the modes corresponding to the O(2) and Ln motions. In fact each of the drawings must be duplicated: one will correspond to the O(2) motion and the
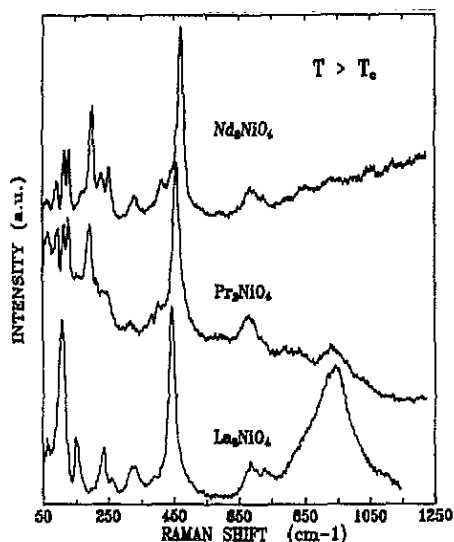
Figure 3. Raman spectra of the stoichiometric Ln$_2$NiO$_4$ compounds at temperatures above their low-temperature structural phase transition.
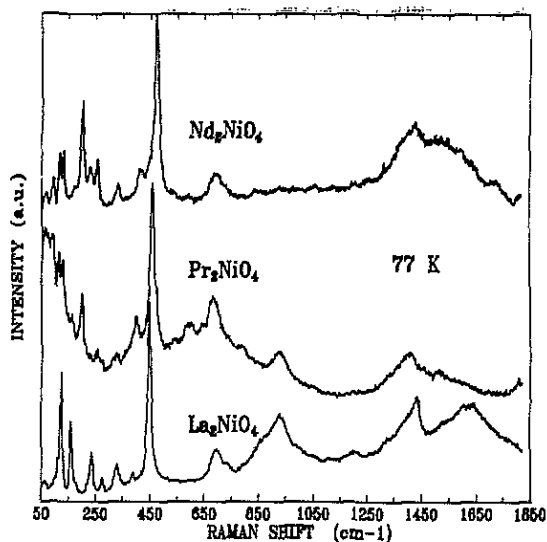
Figure 4. Raman spectra of the stoichiometric Ln$_2$NiO$_4$ compounds at temperatures below their low-temperature structural phase transition.

other to the Ln motion (this is indicated in parentheses after the mode symmetry), while, in the figure, only one has been drawn. These modes consist in stretchings and bendings of the Ln—O(2)—Ni bonds in phase and out of phase of the ions of the two formulae in the primitive cell. Again, the A$_g$(5) (Ln) and A$_g$(4) (O(2)) correspond to the deformation suffered in the tetragonal-to-orthorhombic distortion.

Pintchovius *et al* [6] have observed, at 53 cm^{-1} by neutron scattering in tetragonal La$_{1.9}$NiO$_{3.87}$, the mode at the X point that will correspond to the 'soft mode' of a tetragonal-to-orthorhombic structural phase transition. This soft mode is the combination of the A$_g$(1), A$_g$(5) and A$_g$(4) modes which are now, in the orthorhombic phase, at the Γ point because the primitive cell is doubled at this phase transition and are, therefore, Raman active. While no tetragonal-to-orthorhombic transition occurs in the oxidized samples, it has been clearly observed at approximately 770 K in the stoichiometric La$_2$NiO$_4$.

The Raman spectra of the three compounds at a temperature higher than, but near to, the low-temperature structural phase transition are shown in figure 3. Our samples are ceramics and so no selection rules can be observed; nevertheless it is possible to assign with some reliability the observed peaks to the general ionic motions described before. The way to do this is to compare with previous phonon frequency calculations for tetragonal samples [6, 16] and to observe the systematic phonon behaviour in the three compounds. The orthorhombic distortion is not strong and so it is expected that the most intense peaks will correspond to those observed for the tetragonal related materials.

The allowed vibrations in the high symmetric *I4/mmm* phase are some O(2) and Ln motions while the O(1) vibrations are only allowed in the orthorhombic structure; then, a lower intensity will correspond to these as can be observed in figure 3. In table 1 we collect together the observed phonon frequencies above and below the phase transition and the mode assignment for the three stoichiometric samples. The normal-mode frequency calculations for tetragonal La$_2$NiO$_{4+\delta}$ from [16] are shown in the first column

Table 1. Observed phonon frequencies of the stoichiometric compounds and the mode assignments.

[16], 300 K	La$_2$NiO$_4$ 230 K	La$_2$NiO$_4$ 74 K	Pr$_2$NiO$_4$ 150 K	Pr$_2$NiO$_4$ 74 K	Nd$_2$NiO$_4$ 150 K	Nd$_2$NiO$_4$ 74 K	
E$_g$	63	61	65	63	65	69	δ O(1)
83	87	88	94	88	93	94	$\delta(y)$ Ln, O(2)
E$_u$	109	100	112	114	115	116	$\delta(x)$ Ln
124		111	127	128	129	130	
A$_{1g}$	151	160	160	164	170	171	ν Ln
150	169	178	191	198	199	200	
E$_u$, E$_g$	235	235	213	229	228	228	$\delta(x)$ O(2)
220	263	275	240	254	254	254	
252				274			
B$_{2u}$, E$_u$	335	338	320	312	317	320	δ O(1)
275, 359				326	333	333	
A$_g$	387	389	401	400	412	414	ν O(2)
450	443	445	457	456	470	471	
E$_u$	685	691	679	641	686	690	ν O(1)
652				682		731	
		732	720		725	772	
	946	874	931	923	—	—	2ν_u O(2)
		927					
	1400	1432	1400	1400	1418	1423	2ν O(1)
			1455	1456		1520	

of table 1 for comparison. Odd vibrations are also included because they may be indicative of the frequencies of the corresponding even allowed modes in the ortho-rhombic phase.

The most intense peak at around 450 cm^{-1} is related to the O(2) stretching modes (A$_g$(2) and B$_{3g}$(3)) in a similar way as for other materials: 430 cm^{-1} for La$_{1.85}$Sr$_{0.15}$CuO$_4$ [17] or 450 cm^{-1} for tetragonal La$_2$NiO$_4$ [6]. Its frequency dependence on the compound (La, 443 cm^{-1}; Pr, 457 cm^{-1}; Nd, 470 cm^{-1}) is not due, as could be expected, to a change in the Ni–O(2) distance which is nearly constant (table 2), but to the effect of the shortening of the Ln–O(2) distance induced by decreasing the lanthanide ionic radius as reflected by the increase in the parameter c. The same phonon, but associated with the Ln motions, will be shifted in a similar way but at a lower frequency at around $\omega_{Ln} = \omega_{O(2)}\sqrt{m_O/m_{Ln}}$. The square root mass ratio is about 3 for the three materials; so the frequency will lie at around 150–160 cm^{-1}. We have assigned the peaks in the 150–200 cm^{-1} region to Ln stretching modes.

The bending modes of the O(2) and Ln ions can be separated into motions along the x and y directions. Those parallel to the y axis will correspond to the tetragonal-to-orthorhombic deformation and will have a lower energy than the others. Moreover, the stretching and bending motions of the same ions in a molecule are frequently related by the empiric relation $\omega_s = 2\omega_b$. Then, we have assigned the two peaks in the 220–275 cm^{-1} region to the B$_{2g}$(3) and B$_{1g}$(2) O(2) bending modes. The equivalent Ln bendings are

Table 2. Bond distances and cell parameters above and below the phase transition.

	La$_2$NiO$_4$		Pr$_2$NiO$_4$		Nd$_2$NiO$_4$	
	Bmab	*P4$_2$/ncm*	*Bmab*	*P4$_2$/ncn*	*Bmab*	*P4$_2$/ncm*
a (Å)	5.450	5.500	5.404	5.492	5.381	5.480
b (Å)	5.528		5.578		5.585	
c (Å)	12.512	12.505	12.220	12.157	12.114	12.057
Ni–O(1) (Å)	1.944	1.947	1.950	1.945	1.95	1.952
Ni–O(1') (Å)		1.952		1.974		1.967
Ni–O(2) (Å)	2.235	2.228	2.23	2.21	2.25	2.21
Ln–O(1) (Å)	2.540	2.526	2.50	2.44	2.57	2.45
Ln–O(1') (Å)		2.517		2.57		2.56
Ln–O(2) (Å)	2.338	2.355	2.30	2.28	2.262	2.25

attributed to the 100–130 cm^{-1} zone by comparison with the similar E_u mode at 124 cm^{-1} in tetragonal La$_2$NiO$_4$. However, we have no further arguments to support this assignment.

The highest-energy one-phonon peaks are at around 680 cm^{-1} and must be due to the Ni—O(1) stretchings (breathing mode $B_{3g}(1)$ and quadrupole motion $B_{2g}(1)$) because it is the smallest bond length in the lattice and corresponds to the lightest ions. The frequencies are nearly identical in the three compounds as these compounds have very slight differences in the Ni–O(1) distances (see table 2). In the tetragonal compounds, odd O(1) stretching modes have been reported at these frequencies in the IR spectra [18, 19]. The corresponding bending modes which satisfy the relation $\omega_s = 2\omega_b$ quite well are in the region 310–355 cm^{-1} and can be the $B_{3g}(2)$ and $B_{2g}(2)$ modes. The observed frequencies are in good agreement with the near-invariance of the Ni–O distances in the octahedra.

The low-frequency region is not so clear to interpret because it corresponds to a large number of modes. As we have established before, the lowest-energy modes will correspond to the tilts of the O(1) squares, to the O(2) bendings ($A_g(4)$ and $B_{3g}(5)$) and to the Ln bendings ($A_g(5)$ and $B_{3g}(6)$).

Above the one-phonon region (0–750 cm^{-1}), several features appear in the spectra at around 930 cm^{-1} and in the 1350–1750 cm^{-1} region (figure 4). In La$_2$NiO$_4$ an intense and broad double peak appears at the same position (946 cm^{-1}) as in the oxidized La$_2$NiO$_{4+\delta}$ tetragonal sample (see figure 6) but with a lower relative intensity. In the two compounds ($\delta = 0$ and 0.15) the intensity of this band, relative to that of the one-phonon peaks, decreases with increasing temperature, suggesting a two-phonon character. This band is probably due to odd double phonons allowed by the presence of defects and enhanced by the strong electron–phonon interaction. The defects can be interstitial oxygen ions as reported in these compounds [3, 20]. The corresponding one-phonon frequency (473 cm^{-1}) is very close to the observed O(2) stretching at 443 cm^{-1} and it can be its IR Davydov partner. For Pr$_2$NiO$_4$ there is also a weak peak at 931 cm^{-1} that could have the same origin while for Nd$_2$NiO$_4$ no peak appears.

On examination of the orthorhombic La$_2$NiO$_4$ sample surface, some small black points can be seen. These points should correspond to oxidized tetragonal material with a high number of interstitial oxygen ions that could be the origin of this wide band.

A peak at around 1400 cm^{-1} is present in the three compounds and double phonons of the even O(1) stretching mode can also be seen as has been observed for the cuprates

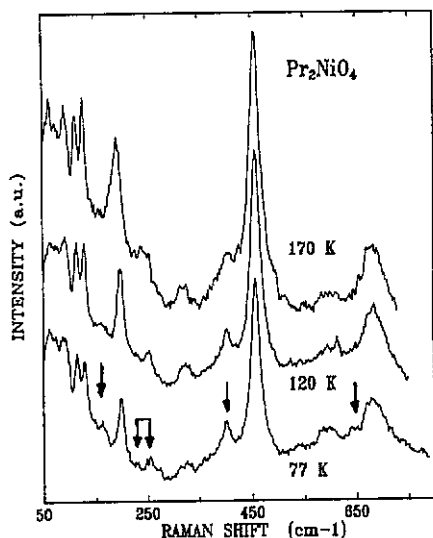**Figure 5.** Raman spectra of Pr_2NiO_4 at three different temperatures. The structural phase transition temperature is at 115 K.
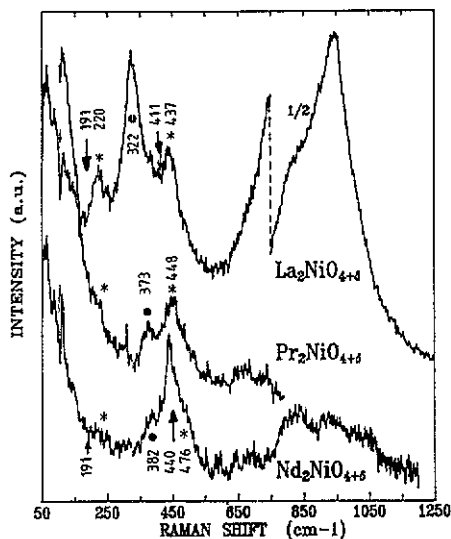
Figure 6. Raman spectra of the oxidized $Ln_2NiO_{4+\delta}$ compounds. The asterisks indicate the Ni–O(2) modes, the arrows the positions of the Ln_2O_3 phonons and the full circles the peaks probably due to modes induced by interstitial oxygen ions.

[9]; however, in this case the intensity does not clearly decrease with increasing temperature. The observed energy shifts of all the described features of the spectra are independent of the exciting beam energy; this rules out the possible luminescence origin of some of these peaks.

The effect of the phase transition on the Raman spectra of the three compounds is very slight, as can be seen by comparing figures 3 and 4. In fact, the high- and low-temperature structures are very similar. The number of Raman modes is doubled principally because the number of ions in the primitive cell is doubled, but this leads basically to 'in-phase' and 'out-of-phase' combinations of the high-temperature modes so that the corresponding frequencies will not be very different and, in many cases, even degenerate. The most affected modes must be those associated with O(1) motions because in the low-temperature phase there are two Ni–O(1) distances.

Figure 5 shows the dependence of the Pr compound Raman spectrum on the temperature. The transition temperature is at 115 K and some new modes and slight peak splittings can be observed (arrows in the figure). Nevertheless, we cannot make any conclusive analysis on the low-temperature phase. There is, undoubtedly, local heating of the sample by the laser beam so that the actual temperature is not known. If we take into account that the lowest temperature at which the spectra have been obtained is around 74 K, it is even possible that the sample local temperature is not very much below the phase transition temperature.

4.2. Oxidized compounds

The lattice vibrational modes for the tetragonal $I4/mmm$ structure have already been described [6, 16]; however, there are only a few Raman studies on the La compound

and none, to our knowledge, on the Pr and Nd nickelates. Recently, Burns and Dacol [14] have shown that some previously reported Raman results for tetragonal $La_{2-x}Sr_xCuO_4$ and La_2NiO_4 are due to locally decomposed material and in particular to La_2O_3. These spectra present peaks at frequencies always lower than those of the corresponding Ln oxides and, for the same lanthanum ion, they depend not only on the other cation (Ni or Cu) but also on the particular sample measured. This would mean that the Ln_2O_3 formed is expanded and, in any case, strongly affected by the matrix. This can be understood only if the Ln oxide precipitates have a very small size (some tenths of an ångström) but is less probable if their dimension is of the order of the spot of the incident beam (some microns).

Anyway, the Ni–O(2) and Ni–Ln distances of the oxidized and stoichiometric samples are very similar and, even if the symmetries are different, the Raman modes active in the more symmetric phase, which are stretchings and bendings of the Ni—O(2)—Ln bonds, must have very similar values for the two phases. For this reason, we expect to find the Ni—O(2) stretching peak at around $450\ cm^{-1}$, its bending mode at around $230\ cm^{-1}$ and the Ln—O(2) stretching at around $180-200\ cm^{-1}$. The oxidized compounds, in opposition to the previously described stoichiometric compounds, present an intense tail towards the elastic line which prevents us from scanning at small frequency shifts. The intensity and quality of the spectra are quite low, probably because of the screening effect of the free charges and because of strong coupling to the lattice vibrations.

Probably some of the peaks of the oxidized sample spectra (figure 6) will correspond to some kinds of defect, obviously present in a high proportion in samples with 15% excess oxygen. These defects could possibly be microparticles of the reported Ln_2O_3 or some other aggregates with different combinations of the elements. These aggregates could be induced by the local increase in the sample temperature and can give rise to their own Raman modes. The other option is point defects, such as interstitial oxygen ions, that can activate some forbidden modes of the lattice or can produce new oxygen vibrations. All these processes can happen and, depending on the history of the sample and on the experimental conditions under which the Raman measurements were carried out, the final results will be different.

In this work the samples were immersed in helium exchange gas at 100 Torr and 150 K and the beam power was always very low; in that way, the possibility of burning the sample was quite reduced. Figure 6 shows the Raman spectra obtained for the three compounds and the lanthanum oxide frequencies are indicated. The peaks assigned to the Ni—O(2) stretchings have frequencies always higher than those for Ln_2O_3 reported in [14]. The Ni—O(2) bending is only clearly seen for the La compound. The rather intense peak at around $330-380\ cm^{-1}$ is most probably due to the activation of vibrations involving the O(1), O(2) and the interstitial oxygen ions, which have been found in the $(\frac{1}{4}, \frac{1}{4}, \frac{1}{4})$ position [3, 20]. The high-frequency peaks at around $950\ cm^{-1}$ have already been discussed for the stoichiometric samples and have probably the same origin.

5. Conclusions

The factor group analysis of the different phases of the stoichiometric Ln_2NiO_4 (Ln $\equiv$ La, Pr, Nd) compounds agrees well with the observed phonons which have been identified with particular atomic movements. The Ni–O distances are nearly equal for all the studied compounds; this explains why the energy of the modes involving O(1) are

basically independent of the rare-earth ion while the Ni—O(2) stretching frequencies are dominated by the variation in the O(2)–Ln distance. The observed double phonons indicate the presence of some defects in the lattice and a strong electron–phonon coupling in these compounds. In the partially oxidized compounds, only two modes have been identified together with some features very probably associated with interstitial oxygen ions.

The observed changes in the Raman spectra of the stoichiometric compounds by decreasing the temperature to 77 K are quite small. We explain this fact because, on the one hand, the expected effect would be the appearance of several peaks at frequencies very similar to the RT peaks and, on the other hand, the local temperature of the sample at the incident beam position can be several tenths of a kelvin higher than the measured temperature, preventing the structural phase transition. The study of the low-energy part of the spectra at lower temperatures with a higher resolution and with single crystals would allow us to observe the soft mode of the phase transition. More work on single crystals is therefore necessary to proceed further with respect to the dynamical properties of these compounds. One interesting question is to understand why the excess of oxygen stabilizes the more symmetric structure.

References

[1] Rodriguez-Carvajal J, Fernandez-Diaz M T, Martinez J L, Fernandez F and Saez-Puche R 1990 *Europhys. Lett.* **11** 261
[2] Fernandez-Diaz M T, Rodriguez-Carvajal J, Martinez J L, Fernandez F and Saez-Puche R 1991 *Z. Phys.* B **82** 275
[3] Rodriguez-Carvajal J, Fernandez-Diaz M T and Martinez J L 1991 *J. Phys.: Condens. Matter* **3** 3215
[4] Rodriguez-Carvajal J, Martinez J L, Pannetier J and Saez-Puche R 1988 *Phys. Rev.* B **38** 7148
   Saez-Puche R, Fernandez F, Martinez J L and Rodriguez-Carvajal J 1989 *J. Less-Common Met.* **149** 357
[5] Birgeneau R J, Chen C Y, Gabbe D R, Jenssen H P, Kastner M A, Peters C J, Picone P J, Thio T, Thurston T R, Tuller H L, Axe J D, Böni P and Shirane G 1987 *Phys. Rev. Lett.* **59** 1329
   Böni P, Axe J D, Shirane G, Birgeneau R J, Gabbe D R, Jenssen H P, Kastner M A, Peters C J, Picone P J and Thurston T R 1988 *Phys. Rev.* B **38** 185
[6] Pintchovius L, Bassat J M, Odier P, Gervais F, Chevrier G, Reichardt W and Gompf F 1989 *Phys. Rev.* B **40** 2229
   Pintchovius L, Bassat J M, Odier P, Gervais F and Reichardt W 1988 *Europhys. Lett.* **5** 247
[7] Mostoller M, Zhang J, Rao A M and Eklund P C 1990 *Phys. Rev.* B **41** 6488
[8] Sulewski P E, Fleury P A and Lyons K B 1990 *Phys. Rev.* B **41** 225
[9] Sugai S, Kobayashi T and Akimitsu J 1989 *Phys. Rev.* B **40** 2686
[10] Axe J D, Moudden A H, Hohlwein D, Cox D E, Mohanty K M, Moodenbaugh A R and Xu Y 1989 *Phys. Rev. Lett.* **62** 2751
[11] Yamada K, Matsuda M, Endoh Y, Keimer B, Birgeneau R J, Onoreda S, Mizusaki J, Matsuura T and Shirane G 1989 *Phys. Rev.* B **39** 2336
[12] Fernandez F, Saez-Puche R, Fernandez-Diaz M T, Rodriguez-Carvajal J, Martinez J L, Botto I L and Baran E J 1991 *Eur. J. Inorg. Solid State Chem.* T **28** 510
[13] Ogita N, Udagawa M, Kojima K and Ohbayashi K 1988 *J. Phys. Soc. Japan* **57** 3932
[14] Burns G and Dacol F H 1990 *Phys. Rev.* B **41** 4747
[15] Kourouklis G A, Jayaraman A, Weber W, Remeika J P, Espinosa G P, Cooper A S and Maines R G 1987 *Phys. Rev.* B **36** 7218
[16] Bates F and Eldridge J E 1989 *Solid State Commun.* **72** 187
[17] Burns G, Dacol F and Shafer M W 1987 *Solid State Commun.* **62** 687
[18] Gervais F, Echegut P, Bassat J M and Odier P 1988 *Phys. Rev.* B **37** 9364
[19] Bazhenov A V, Fursova T N, Timofeev V B, Cooper A S, Remeika J P and Fisk Z 1989 *Phys. Rev.* B **40** 4413
[20] Jorgensen J D, Dabrowski B, Pei S, Richards D R and Hinks D G 1989 *Phys. Rev.* B **40** 2187